

I Load measurements in reinforced concrete columns

Jaime Tupiassú Pinho de Castro, Ronaldo Domingues Vieira
Department of Mechanical Engineering, Pontifical Catholic University of Rio de Janeiro, Rio de Janeiro/RJ – Brazil

Rafael Araújo de Sousa
Department of Civil Engineering, Pontifical Catholic University of Rio de Janeiro, Rio de Janeiro/RJ – Brazil

Marco Antonio Meggiolaro, José Luiz de França Freire
Department of Mechanical Engineering, Pontifical Catholic University of Rio de Janeiro, Rio de Janeiro/RJ – Brazil

Abstract

Particularly careful strain measurements made on several reinforced concrete columns yielded much higher values than initially expected, causing great concern since their final objective was to evaluate the forces that were loading the columns. Indeed, some loads calculated from the measured strain in a standard linear elastic way appear to be larger than the column's ultimate design load. However, despite its widespread use in structural design, such linear elastic calculations do not include the very significant influence of concrete creep on the columns strain state, a phenomenon that is only implicitly considered by the "allowable stresses" specified in their design codes. Since this procedure is inappropriate for experimental stress analysis purposes, a relatively simple viscoelastic model is proposed to describe the concrete long term stress-strain behavior. This model is extended to describe the reinforced columns behavior, and then qualified by fitting it to concrete column creep data from the literature, proving that despite their high value the measured strains were indeed compatible with the columns load history.

Keywords: concrete creep, residual stresses, time-dependent strain measurements.

1 Introduction

A large and very busy subway station was suffering important structural modifications to serve as the main commuting point between an existing line and a new one under construction. That station was originally conceived as a crossing point, but in its original plan the new subway line would have two parallel tunnels to hold its two railways, and its structure was accordingly built several years ago.

21 However, that original plan had to be changed, as the new line was being dug by a machine which
22 opened a larger hole to hold the two railways inside a single tunnel. Consequently, several columns
23 of that veteran station should be removed and properly replaced to allow the passage of the digging
24 machine, and the settlement of the new line with its adjacent railways. Moreover, this unusual task
25 should be fulfilled without interrupting the old line regular transportation services. To assure the
26 safety of this process, load measurements were specified in all the columns that would be removed or
27 could be affected during the station upgrade.

28 Direct load measurements were impossible in this case, not only because the reinforced concrete
29 columns were built into the subway station structure, but also because it should continuously support
30 the existing line traffic without interruptions during the whole construction campaign of the new line.
31 In view of his limitation, residual or resident strain measurements by localized stress releases were
32 proposed as an alternative method for indirectly measuring the required loads, which should of course
33 be calculated from the strain measurements by using the appropriate columns stiffness properties.

34 The around 1.2m diameter concrete columns were reinforced by some 30 or more vertical steel rods,
35 tied in a standardized way. The rods diameters were either 16, 20 or 24mm, depending on the column
36 design load. The steel rods had a minimum yield strain $\epsilon_{Ymin} > 2500\mu m/m$, and were distributed more
37 or less circumferentially near the columns perimeter in approximately uniform intervals. But there
38 was no warranty about the depth of the rods, nor about the thickness of the concrete layer which
39 covered them. This thickness, as it was later on verified, indeed varied significantly from column to
40 column, and even around a same column.

41 To avoid the uncertainty associated with residual strain measurements made on concrete layers of
42 varying thickness, four small windows were opened on most columns, to expose a small portion of
43 some of their steel reinforcing bars, see Figure1. The windows on the columns surfaces were spaced
44 at approximately 90° and opened in a same transversal plane. The reinforcing bars were strain-gaged
45 and then sectioned to alleviate their service strains. Note that instead of using only three co-planar
46 measurement points, which is the minimum number required to separate the normal from the bending
47 strains, whenever possible four reinforcing bars were instrumented in each column to provide some
48 measurement redundancy. This conservative practice is strongly recommendable, not only to avoid
49 losing important information in case of an eventual gage problem, but also to provide some insight on
50 the measurement dispersion. Due to the severe structural risk problem associated with the columns
51 removal, this measurement service was made with particular care by highly trained personnel.

52 In a few columns, only three windows could be opened, due to access limitations, losing in this
53 way the redundancy discussed above, but still allowing the separation of the normal from the bending
54 loads. The windows were typically around 200mm high, and their depth and horizontal size were
55 kept as small as possible (around 150mm wide with a 50 to 100mm depth, see Fig.1) to allow the
56 preparation of the rod's surface for bonding the strain gage, and the subsequent cut of the lower part
57 of the exposed rod by a 125mm abrasive wheel.

58 A carefully grounded small plane recess was introduced at the superior part of each exposed rod
59 inside the small windows opened around the column, which surface was later on finished by hand
60 using a 220 grid sand paper. In most cases, these plane recesses were about 8 to 12mm wide and 40
61 to 60mm long. After proper cleaning the sanded recess surface, a uniaxial strain gage was bonded on

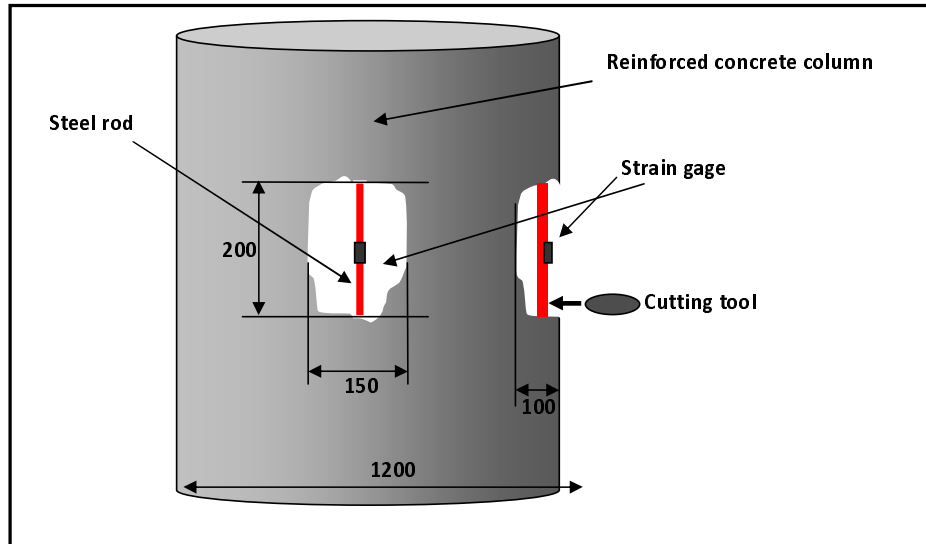


Figure 1: Sketch of the residual or resident strain measurement procedure.

62 it using a cyanoacrilate adhesive. The gages were then connected to a three wire shielded cable, and
63 finally protected by a neutral silicone rubber barrier.

64 To make the residual strain measurements, after having bonded, cabled and protected all the four
65 gages (or three, if one side of the column was not accessible) of a column, they were simultaneously
66 connected to a precision four channel portable strain indicator, and properly balanced. Then the lower
67 part of the rods were slowly cut by the abrasive wheel, always in several steps to allow for proper
68 water cooling during the progressive cutting, in order to avoid overheating the gage (this task was
69 easily achieved by holding the rods with a bare hand). The cuts were always performed at least 100mm
70 (or more than 4 to 5 rod diameters) from the gage, and the strain readings were only made after the
71 complete stabilization of their (small) thermal transients.

72 It is worth mentioning that if the concrete layers over the rods were sufficiently thick, or if the
73 columns were made of non-reinforced concrete, the rod sectioning method could be substituted by the
74 tick-tack-toe method proposed elsewhere [1].

75 Despite all the care, the measured results turned out to be much higher than initially expected, a
76 big problem for the engineers in charge of the expansion project. Thus, the first reaction of the experts
77 on concrete structures, who should in principle provide the columns stiffness properties necessary for
78 the loadings calculations, was to question the accuracy of the strain measurements. This questioning
79 was an irrefutable and welcome challenge for the measuring team, whose solution turned out to be
80 quite interesting, as shown in the following sections.

2 Strain measurements

Before starting any analysis, it is important to point out that the released strain measured in any steel rod of a reinforced concrete column can in general be due to the superposition of several mechanisms, namely:

1. the rod service stress, which is caused by the column load (remembering that this load, whose evaluation is the final objective of such a measurement, generally has both a compression and a bending component);
2. concrete creep under the service load (the steel rods do not creep significantly at room temperature, but their strain also increase as time passes by to maintain their geometrical compatibility with the slowly creeping concrete);
3. concrete shrinkage during its cure (whose consequences are similar to creep);
4. residual stresses introduced during the rods' manufacturing (e.g. by non-uniform plastic deformations and/or heat treatments);
5. residual stresses introduced during the mounting of the reinforcement (by bending, torsion and/or tying of the reinforcing rods);
6. concrete removal to expose the rod for the measuring process (the load carried by that small volume is partially transferred to the exposed rod); and
7. rod cross section decrease during the preparation of its surface for bonding the gage (if the rod load is constant, its stress and strain increase as the cross section decreases).

The severance of any rod interrupts its force path and, as a result, completely releases all these strain components under the gage, no matter which mechanisms caused them. This strain alleviation can be correlated with the rod stress, and thus with the forces that were imposed in the rod to cause it, if:

1. it can be supposed that the stress caused by the load in the rod is uniaxial, a quite reasonable assumption in such a slender member built into a concrete column of a much larger diameter; and
2. all the other strain parcels can be neglected or properly evaluated.

Since the rod sectioning cuts where always made several rod diameters from the gages, the residual stresses eventually (and usually) introduced during the rods manufacture, which are of course self-equilibrating in any cross section, should not significantly affect the gage measurements according to Saint Venant's principle. Consequently, component 4 of the above list could be safely neglected when analyzing the total released strain.

As all 4 (or 3) gages of a given column were continuously monitored during the cutting process, it could be observed that cutting a rod did not influence the others, whose signals remained balanced within the strain indicator noise level (always less than $5\mu\text{m}/\text{m}$). Therefore, the column stiffness loss introduced by alleviating the instrumented rods was negligible, and so was the 6th listed component of the total rod strain.

All the exposed rods were checked for lateral displacements and/or rotations after the cuts, but they maintained the alignment in almost all cases, evidence that the mounting stresses which could cause the 5th listed strain component were also negligible.

121 Finally, the effect of the rod cross section reduction, necessary for mounting the gage, could easily
 122 be accounted for, as schematized in Figure 2. The grinding of a short and small plane recess on the
 123 rods surface was needed to bond the gage (because reinforced rods have a very rough surface and a
 124 helical external thread for improving their adherence to the concrete), but they not only reduced the
 125 rod cross section, as they also introduced some local bending due to the eccentricity of their (assumed)
 126 pure compression load.

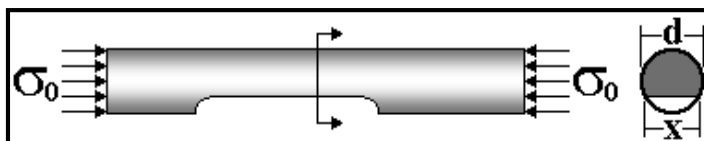


Figure 2: The small recess for bonding the gages introduces some bending strains in the rod.

127 The exposed part of the rod is really loaded under displacement control, since its strain is imposed
 128 by the rest of the column, which is much stiffer than the rods. However, since the recess was small
 129 and short, it can be modeled as if it was loaded under a pure axial load which induced a stress σ_0 on
 130 its section.

131 Thus, if σ_0 is the pure nominal compression stress acting on the original section of a reinforcing
 132 rod of diameter d and area $A_0 = \pi d^2/4$, x is the width of the recess, and $A = d^2(\alpha - \sin\alpha \cdot \cos\alpha)/4$ is the
 133 area of the plane recess section, where $\alpha = \pi \sin(x/d)$, then the stress σ under the gage (which has a
 134 normal and a bending component) is given by (see Figure 3):

$$\sigma = \frac{32\sigma_0 A_0}{3d^2} \left\{ \frac{\frac{(\sin \alpha)^3}{(\alpha - \sin \alpha \cdot \cos \alpha)} \left[\frac{2(\sin \alpha)^3}{3(\alpha - \sin \alpha \cdot \cos \alpha)} - \cos \alpha \right]}{\alpha - \sin \alpha \cdot \cos \alpha + 2(\sin \alpha)^3 \cdot \cos \alpha - \frac{16(\sin \alpha)^6}{9(\alpha - \sin \alpha \cdot \cos \alpha)}} + \frac{1}{A} \right\} \quad (1)$$

135 The mean value of the released strains measured after having cut more than 100 reinforcing rods
 136 of 28 different columns was $\epsilon_m = 1325 \mu\text{m}/\text{m}$, and the maximum was $\epsilon_{max} = 2600 \mu\text{m}/\text{m}$. Thus, most
 137 measured strains were still within the linear elastic range of the steel rods, except for ϵ_{max} that was
 138 slight above ϵ_{Ymin} . But they indeed seem to be too large for the concrete, whose ultimate design strain
 139 is generally taken as $\epsilon_U = 2000 \mu\text{m}/\text{m}$. No prudent structural engineer would ever want to approach
 140 such a value under the maximum load conceived for his or her design. Even after considering the
 141 recess correction, which decreased the measured strain values in average by 20%, in a first look they
 142 still seems to imply that the columns were or could be unsafe. But there was no other evidence of
 143 such a problem, since no cracking, screaming or any other warning was ever emitted by the columns,
 144 even after opening the windows to expose the rods. As a result, it was much simpler to just dismiss
 145 the measurements, assuming they were simply wrong.

146 On the other hand, there was no evidence of any problem with the measured strains. The measure-
 147 ments followed reliable and very well established procedures, including electrical tests of the reading

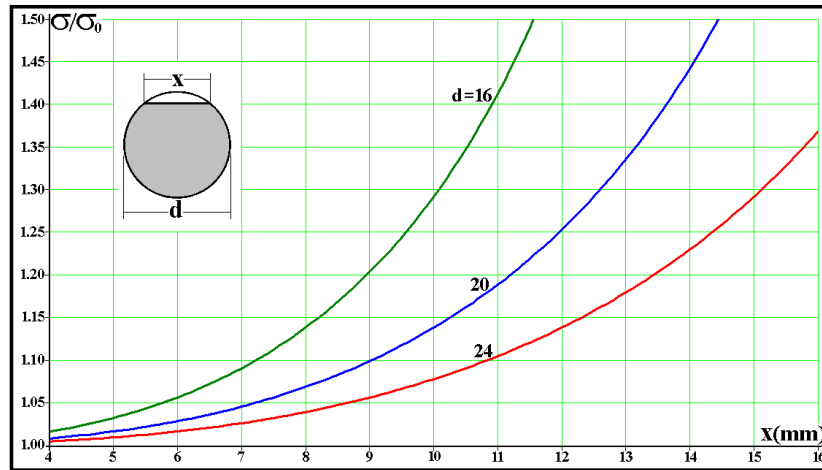


Figure 3: Ratio σ/σ_0 as a function of the recess width x for the three rod diameters: this effect is not negligible in most cases, and it must be accounted for in the load analysis.

148 equipment with high precision resistors and operational tests of the installed gages, always generat-
 149 ing consistent checks. Moreover, as the tests were made by veteran engineers with a long practical
 150 experience in the field and a sound theoretical background, their qualitative opinion is an asset that
 151 cannot be ignored. Therefore, something had to be done to make sense out of these two apparently
 152 incompatible, but very strong evidences, as explained below.

153 3 The viscoelastic behavior of concrete

154 Concrete is made by mixing gravel, sand and a calcium silicate cement powder, which are all ceramic
 155 materials, with water, which hydrates and hardens the cement to form a rock-like composite. Therefore,
 156 it may sound strange to talk about concrete creep at room temperature. Nevertheless, concrete can
 157 creep a lot. For example, Figure 4 shows some concrete creep data presented by Leeth [2]. According
 158 to Buyukozturk [3], concrete creep is influenced by factors that can be internal, dependent on the
 159 concrete composition (such as concentration, stiffness, grading, distribution and permeability of the
 160 aggregate, water/cement ratio, cement type, etc.), or external, dependent on structural parameters
 161 (size, shape, environment, loading, etc.). Moreover, creep strains are linearly proportional to the stress
 162 typically if $\sigma < f'_c/2$, where f'_c is the concrete compressive strength, usually measured after a 28 day
 163 curing time.

164 The three curves shown in Figure 4 show only the creep strains measured under 2.1, 4.2 and 6.3 MPa,
 165 which after 600 days are $\epsilon_{cr} = 446, 872$ and $1325 \mu\text{m}/\text{m}$ (but the total strain has also an initial elastic
 166 part $\epsilon_{el} = \sigma/E = 100, 200$ and $300 \mu\text{m}/\text{m}$, respectively.) Therefore, the creep strains are certainly not
 167 negligible in these tests. Moreover, these creep strains are indeed linearly proportional to the stresses,

168 as shown in Figure 5, where the curves obtained under 2.1 and 4.2MPa practically coincide with the
 169 6.3MPa curve when multiplied by 3 and 1.5, respectively.

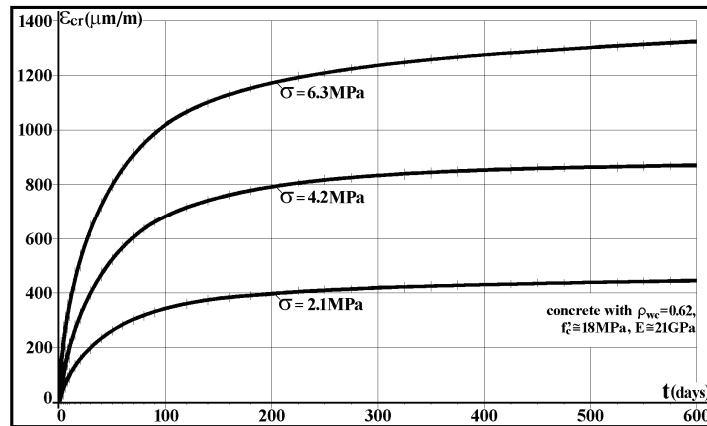


Figure 4: Time variation of creep strains under compressive stresses (plotted as positives for convenience) for a concrete with compressive strength $f'_c = 18MPa$, Young's modulus $E_{c28} \cong 1.36(\rho_c^3 \cdot f'_c)^{0.5} \cong 21GPa$ (both measured, as usual, 28 days after casting), water/cement ratio $\rho_{wc} = 0.62$, and density $\rho_c \cong 2.3$.

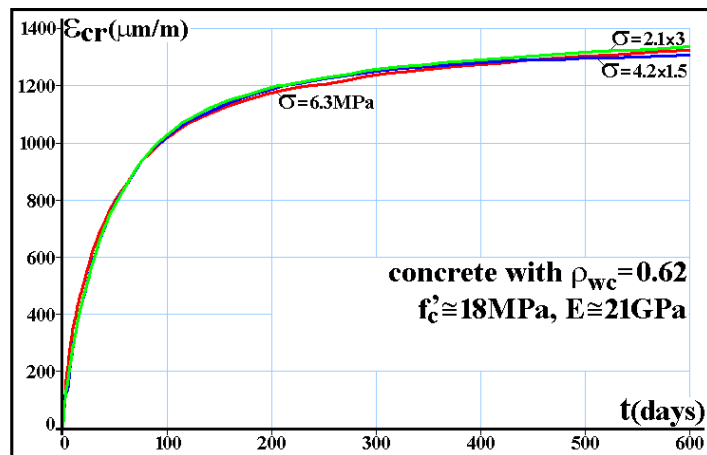


Figure 5: The concrete whose creep curves are shown in Figure 4 is indeed a linear viscoelastic material, since the 3 curves practically coincide when properly scaled by a $6.3/\sigma$ factor.

170 The next step is to find a proper rheological model to reproduce all these curves, which should not
 171 include the elastic strains as they show only the creep strains. A first option could be to try to fit
 172 the data by a Kelvin-Voigt equation, but as the experimental creep data does not show a horizontal
 173 asymptote, at least another damper is needed in the model.

174 A generic non-linear curve can be fitted to a set of data by minimizing its mean square deviation
 175 from that set using, for example, the Levenberg-Marquardt (LM) algorithm [4, 5]: given a set of m
 176 points (x_i, y_i) , $i = 1, \dots, m$, LM searches for the parameter vector $p = [p_1, p_2, \dots, p_n]^T$ (where T means
 177 transpose) containing the n constants of the specified $f(x_i, p)$ function which minimizes the sum of the
 178 square deviations:

$$S(p) = \sum_{i=1}^m [y_i - f(x_i, p)]^2 \quad (2)$$

179 The LM algorithm can be applied to non-linear vectorial functions, whereas x_i can be a scalar
 180 for one-variable functions, or a vector for functions of more than one variable. But in the following
 181 formulation, $f(x_i, p)$ and y_i are supposed scalars. It is didactic to present a few practical applications
 182 of such functions, for example, in fatigue: when using Paris' rule $da/dN = f(x_i, p) = A \cdot \Delta K^m$, $x_i = \Delta K$
 183 and $p = [A, m]^T$; whereas for Walker's rule $da/dN = f(x_i, p) = A_w \Delta K^{m_w} K_{max}^{p_w}$, $x_i = [\Delta K, K_{max}]^T$ and
 184 $p = [A_w, m_w, p_w]^T$; and for Coffin-Manson's rule $\Delta \epsilon = f(x_i, p) = (2\sigma_c/E)(2N)^b + (2\epsilon_c)(2N)^c$, $x_i = N$ and p
 185 $= [\sigma_c, E, b, \epsilon_c, c]^T$.

186 LM is an iterative procedure, which depends on an initial estimate for the vector p , which for highly
 187 non-linear functions needs to be fairly close to the final solution to guarantee convergence. However,
 188 this normally is not the case when fitting data obtained in mechanical tests. In each iteration, p is
 189 replaced by a new estimate $p + q$. To find the vector $q = [q_1, q_2, \dots, q_n]^T$, the functions $f(x_i, p + q)$ are
 190 approximated by their linearizations, given by

$$f(x_i, p + q) \cong f(x_i, p) + J(x_i, p) \cdot q \quad (3)$$

191 where J is the Jacobian of f with respect to p :

$$J(x_i, p) = \left[\frac{\partial f(x_i, p)}{\partial p_1}, \frac{\partial f(x_i, p)}{\partial p_2}, \dots, \frac{\partial f(x_i, p)}{\partial p_n} \right] \quad (4)$$

192 In the case discussed here, as f is scalar, the Jacobian results in the gradient of f with respect to
 193 p . When the sum of the deviations $S(p)$ is minimum, the gradient of S with respect to q is equal to
 194 zero. Therefore, applying equation (2) at $S(p + q)$, and making $\partial S/\partial q = 0$, results in

$$\sum_{i=1}^m \{J(x_i, p)^T \cdot J(x_i, p)\} \cdot q = \sum_{i=1}^m \{J(x_i, p)^T \cdot [y_i - f(x_i, p)]\} \quad (5)$$

195 In this manner, the correction vector q can be obtained in each iteration by:

$$q = \left[\sum_{i=1}^m J(x_i, p)^T \cdot J(x_i, p) \right]^{-1} \cdot \sum_{i=1}^m \{J(x_i, p)^T \cdot [y_i - f(x_i, p)]\} \quad (6)$$

196 All the m experimental data points can be stacked in an $m \times n$ matrix J_t and in an $m \times 1$ error vector
197 e_t , defined as:

$$J_t(p) \equiv \begin{bmatrix} J(x_1, p) \\ J(x_2, p) \\ \vdots \\ J(x_m, p) \end{bmatrix} \quad (7)$$

198 Then, equation (6) can be rewritten as:

$$q = (J_t^T J_t)^{-1} J_t^T \cdot e_t \equiv \text{pinv}(J_t) \cdot e_t \quad (8)$$

199 where $\text{pinv}(J_t)$ is known as the pseudo-inverse of J_t , with $\text{pinv}(J_t) \equiv (J_t^T J_t)^{-1} J_t^T$. After finding q in
200 each iteration and summing it to the current p estimate, the algorithm continues updating p until
201 the correction q has absolute value smaller than a given tolerance.

202 If f varies linearly with p , then J does not depend on p , and the algorithm converges in only one
203 iteration. Even when J depends on p , the use of a log-log scale usually guarantees convergence in a
204 few iterations. It is advisable to monitor the value of the deviation sum $S(p)$, which should always
205 decrease at each iteration. If $S(p)$ increases in some iteration, a possibility when working with highly
206 non-linear functions, it is necessary to introduce a positive damping term λ in the pseudo-inverse:

$$q = (J_t^T J_t + \lambda I)^{-1} J_t^T \cdot e_t \quad (9)$$

207 where I is the identity matrix $n \times n$. The damping factor λ is updated at each iteration. If the $S(p)$
208 reduction is too high, smaller values are chosen for λ to avoid that the algorithm becomes unstable.
209 On the other hand, if $S(p)$ decreases too slowly, λ is increased to accelerate the convergence of the
210 iterative calculations.

211 Marquardt [5] recommends that damping be introduced in the numerical calculation algorithm for
212 calculating the correction vector q by guessing an initial value $\lambda = \lambda_0 > 0$ and a correction factor
213 $v > 1$, e.g. $\lambda = 1$ and $v = 2$. At each iteration, q is calculated using a damping factor λv . If $S(p + q)$
214 $< S(p)$, then this q is summed to p , $\lambda = \lambda v$ is chosen as the new factor, and a new iteration is made.
215 In the opposite case, q is recalculated using λ . If $S(p + q) < S(p)$, then this q is summed to p , λ is
216 maintained, and a new iteration begins. If in both cases $S(p + q) \geq S(p)$, then q is recalculated with
217 damping factors $\lambda \cdot v^k$, $k = 1, 2, \dots$, at each new iteration until obtaining $S(p + q) < S(p)$. When this
218 occurs, then this q is summed to p , $\lambda = \lambda \cdot v^k$ is chosen as the new damping factor, and the iterations
219 continue. With this procedure, the algorithm stability is guaranteed.

220 As shown in Figure 6, two viscoelastic models are used to fit the average of the curves shown in
221 Figure 5, using the above procedures. The first model is Kelvin-Voigt's, with its 2 parameters k and

222 c obtained by minimizing the mean square error, generating curve 1. The second is a Kelvin-Voigt
 223 model in series with a damper, generating curves 2 and 3, either by applying the same method or by
 224 visually re-fitting the parameters c_1 , c_2 and k_2 , respectively. The introduction of a damper in series
 225 with the Kelvin-Voigt element improves the data fitting, but the “optimum” mathematical adjustment
 226 is not as good as the old-fashioned eye-ball data fitting used to obtain curve 3. This visual tuning of
 227 the parameters generated by LM is a much recommended procedure, since there is no substitute for a
 228 well trained human judgment: the eye-ball fitting does not minimize the least square error, however it
 229 ended up fitting better the long-term creep behavior, especially after 500 days. But such a refinement
 230 by man-machine interaction is only possible after knowing the mathematically optimized parameters.
 231 In these cases, it is a particularly powerful tool when working with non-linear functions.

232 The LM generated curve 1 parameters are $k = 5GPa$ and $c = 21.6GPa \cdot s$, whereas for curve 2 the
 233 optimum parameters are $c_1 = 1.196TPa \cdot s$, $k_2 = 5.8GPa$ and $c_2 = 18.92GPa \cdot s$. The subjective final visual
 234 adjustment of curve 3 generates $c_1 = 1.814TPa \cdot s$, $k_2 = 5.8GPa$ e $c_2 = 21.6GPa \cdot s$. But to model the total
 235 concrete strain, another spring $k_1 = 21GPa$ in series with the damper c_1 must be used to simulate the
 236 elastic modulus E_{c28} estimated above, see Figure 7.

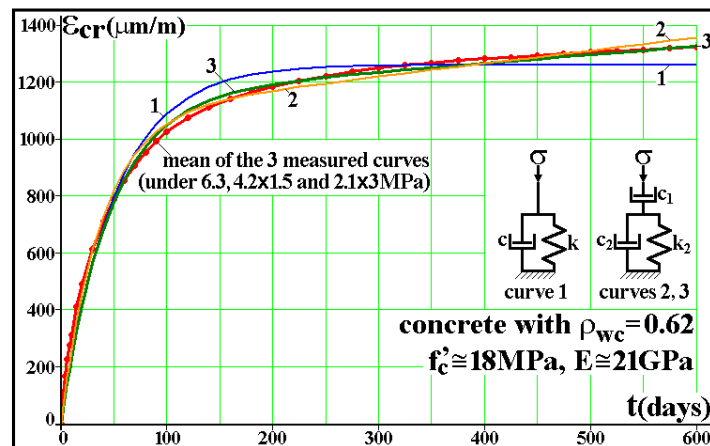


Figure 6: Fitting of the concrete creep data presented in Figure 5.

237 This 4-element Burger model shown in Figure 7 is capable of reproducing well the long term mechan-
 238 ical behavior of the concrete whose creep data is given in Figure 4. However, to model a reinforced
 239 concrete column under pure compression, it is necessary to use still another spring in parallel with
 240 the Burgers model, to describe the effect of the steel rods. Only one spring is needed because the steel
 241 creep can be neglected at room temperature. Also, this spring is in parallel with the concrete model
 242 because both see the same strains to maintain geometric compatibility inside the column.

243 Therefore, if A_s is the total area of the reinforcing steel rods and A_c is the concrete area in a column
 244 whose cross section area $A = A_s + A_c$, then $f_{a_s} = A_s/A$ and $(1 - f_{a_s})$ are the area fractions of the steel

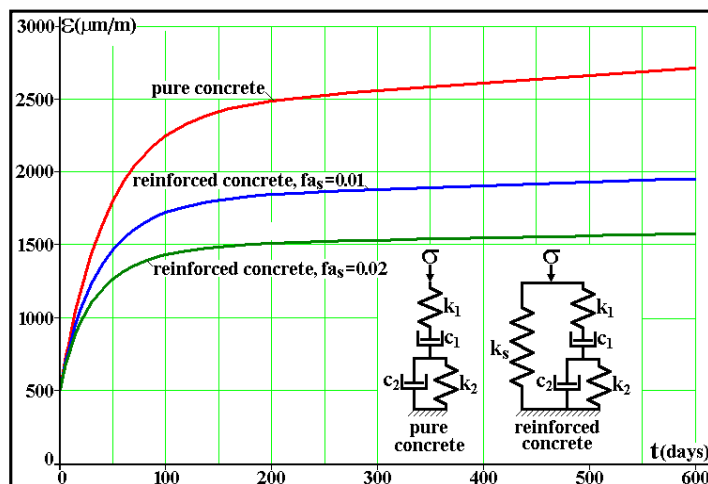


Figure 7: Strain histories $\epsilon(t)$ estimated by equation (10) for a pure concrete and for two steel reinforced concrete columns with steel area fractions $f_{a_s} = 1\%$ and $f_{a_s} = 2\%$, when they are loaded by a fixed force that causes an initial strain $\epsilon_0 = 500\mu\text{m/m}$. The concrete is modeled as a linear viscoelastic Burgers' material with constant parameters $k_1 = 21\text{GPa}$, $c_1 = 1.814\text{TPa}\cdot\text{s}$, $k_2 = 5.8\text{GPa}$ e $c_2 = 21.6\text{GPa}\cdot\text{s}$, whereas the steel reinforcement is modeled as a Hookean material with $k_s = 200\text{GPa}$.

245 and the concrete in the column. If F is the force (supposed constant) which loads the column; E_s
 246 is the steel elastic modulus (which does not creep) and $E_c(t)$ is the (variable) creep modulus of the
 247 concrete; $\sigma_s(t)$ and $\sigma_c(t)$ are the stresses on the rods and on the concrete (both vary in time, since the
 248 concrete creep transfers loads to the steel reinforcing rods); and $\epsilon(t)$ is the column strain (which also
 249 varies as time passes by), then it is trivial to show that the compressive force in the column is $F =$
 250 $\sigma_s(t)\cdot A_s + \sigma_c(t)\cdot A_c = \epsilon(t)\cdot[E_s\cdot A_s + E_c(t)\cdot A_c]$, therefore:

$$\epsilon(t) = \frac{F}{E_s A_s + E_c(t) A_c} = \frac{F/A}{f a_s k_s + \frac{(1-f a_s)}{1/k_1 + t/c_1 + [1 - \exp(-k_2 t/c_2)]/k_2}} \quad (10)$$

251 It is also easy to show that the equivalent stress in the column is given by:

$$\sigma = F/A = \epsilon(0)[f a_s k_s + (1 - f a_s) k_1] = \epsilon_0[f a_s k_s + (1 - f a_s) k_1] \quad (11)$$

252 The steel area in a reinforced concrete column is typically 1 to 2% of its total area. Knowing that
 253 the (elastic) ultimate strain in reinforced concrete structural design is usually assumed as $2000\mu\text{m/m}$,
 254 a column designed for an initial strain $\epsilon_0 = 500\mu\text{m/m}$ can thus be considered representative of the
 255 problems found in practice. Using this value, Figure 7 shows the strain time variations expected from
 256 a pure concrete column (with $f'_c = 18\text{MPa}$ and all the viscoelastic properties obtained above), and

257 from two reinforced concrete columns, one with a steel area fraction $f_{a_s} = 0.01$ and the other with f_{a_s}
258 $= 0.02$.

259 Figure 7 demonstrates that strains in the order of $\epsilon_{max} = 1500$ to $2000\mu m/m$ are certainly not
260 incompatible with typical working loads applied on reinforced columns made out of the concrete
261 whose creep strains are described by Figure 4. But this figure does not include several important
262 details about the concrete properties, which had to be estimated in order to generate the information
263 that supports this claim, a fact that decreases its power. However, a quite comprehensive report by
264 Ziehl et al. [6] presents several such details, removing any doubts about the adequacy of this approach.

265 Ziehl and his colleagues studied if reinforced concrete columns with steel area fractions $f_{a_s} < 1\%$,
266 the minimum steel fraction required by the American standard [7, 8], could be used for structural
267 purposes. They said that those existing minimum f_{a_s} requirements for columns were developed to
268 prevent yielding of the reinforcement resulting from creep deformations in the concrete; that the tests
269 used to support this limit were conducted decades ago, when steel yield strengths for reinforcing bars
270 were approximately half of what is common today; and that a substantial reduction in the column
271 steel area fraction might be possible with present-day materials, resulting in economic savings.

272 Ziehl et al. have cast several $203mm$ (8") diameter by $1219mm$ (4') long cylindrical columns made out
273 of two concretes with nominal compressive strengths (at 28 days) of 28 and $56MPa$ (4 and $8ksi$), with
274 three steel fractions f_{a_s} (0.36, 0.54, and 0.72%). They have subjected them to a constant axial load
275 $F = 0.4 \cdot f'_c \cdot A$ (the maximum load allowed by ACI [8] and AASHTO [9] standards) in reduced-humidity
276 enclosures, and measured their long-term axial deformations using electronic and mechanical strain
277 gages. The load was applied through coil springs, to provide the necessary compliance. Unloaded
278 specimens were used to monitor temperature and shrinkage-related deformations. They presented
279 plots of measured strain versus time, and compared the experimental results with an empirical model
280 reported by the ACI Committee 209 [7].

281 The columns were cast in cardboard molds, which were stripped five days after having poured
282 the concrete. These columns were loaded between 14 and 28 days after casting. To determine the
283 material properties, 4×8 and 6×12 inch test cylinders were also cast for every group of columns.
284 These cylinders were tested for modulus of elasticity and compressive strength at 7, 14, 28, and 56
285 days after casting. The steel rods were tested for yield and ultimate strengths. Dehumidifiers were used
286 to keep the relative humidity and temperature generally between 30 and 60% and 10 and $43^\circ C$. The
287 period required to load the columns for a length of time sufficient for the rate of creep to approach
288 nearly zero was initially estimated to be close to two years, but in practice it was 15 to 18 months,
289 depending on the specimens. Ziehl's report is particularly meticulous, and should be consulted for
290 further details on concrete specifications and experimental procedures. Figures 8-11 show how the
291 technique discussed above can quite reasonably fit some of their data.

292 4 Conclusions

293 A relatively simple linear viscoelastic model was proposed to describe concrete creep, and extended
294 to model the behavior of reinforced columns under axial loading. The model treats the concrete as
295 a Burgers' solid, composed by a Maxwell's element with a spring k_1 (which represents its short term

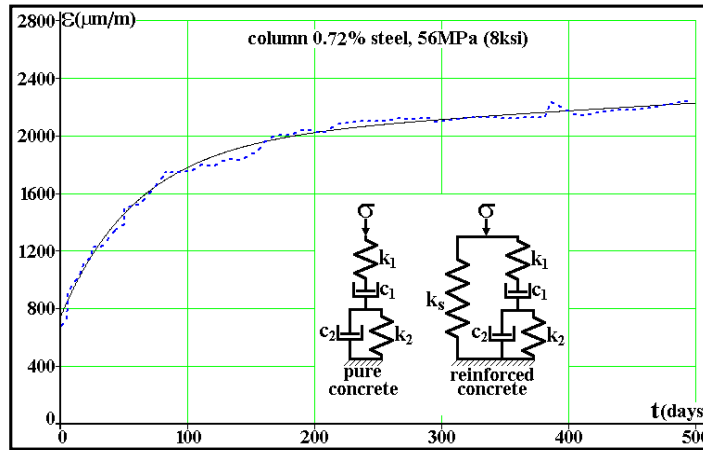


Figure 8: Total (elastic plus creep) strain history $\epsilon(t)$ estimated by equation (10) for a reinforced concrete column with $f'_c = 56\text{MPa}$ and steel area fraction $f_{a_s} = 0.72\%$, loaded by a fixed force that induces an initial (elastic) strain $\epsilon_0 = 800\mu\text{m/m}$ (curve generated by using the fitted viscoelastic parameters $k_1 = 37.54\text{GPa}$, $c_1 = 40\text{TPa}\cdot\text{day}$, $k_2 = 19\text{GPa}$ and $c_2 = 1.2\text{TPa}\cdot\text{day}$.)

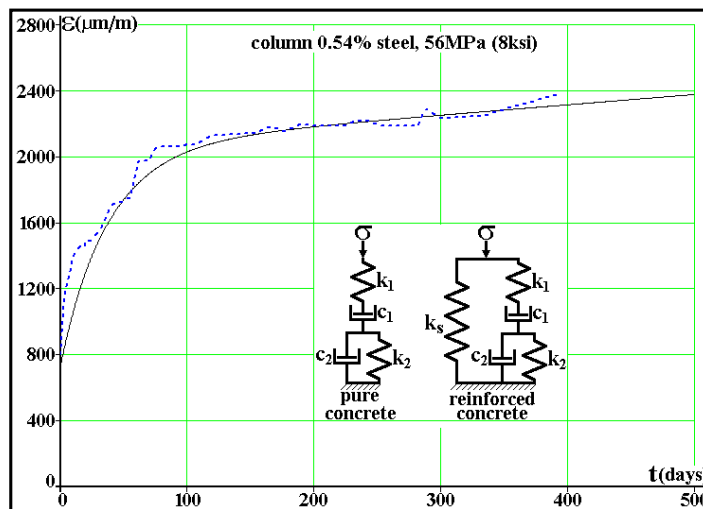


Figure 9: Strain history $\epsilon(t)$ for a $f'_c = 56\text{MPa}$ reinforced concrete column with steel area fraction $f_{a_s} = 0.54\%$, loaded by a force that causes an initial strain $\epsilon_0 = 800\mu\text{m/m}$ (curve generated using $k_1 = 24.87\text{GPa}$, $c_1 = 80\text{TPa}\cdot\text{day}$, $k_2 = 6.5\text{GPa}$ and $c_2 = 340\text{GPa}\cdot\text{day}$.)

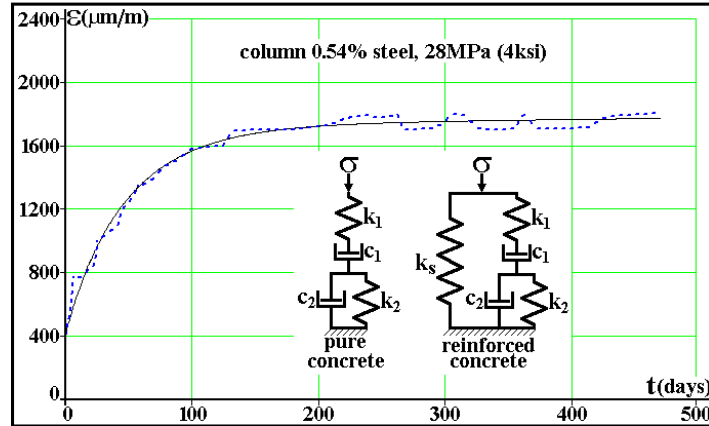


Figure 10: Strain history $\epsilon(t)$ for a $f'_c = 28\text{MPa}$ reinforced concrete column with steel area fraction $f_{a_s} = 0.54\%$, loaded by a fixed force that induces an initial strain $\epsilon_0 = 400\mu\text{m/m}$ ($k_1 = 24.87\text{GPa}$, $c_1 = 80\text{TPa}\cdot\text{day}$, $k_2 = 6.5\text{GPa}$ and $c_2 = 340\text{GPa}\cdot\text{day}$.)

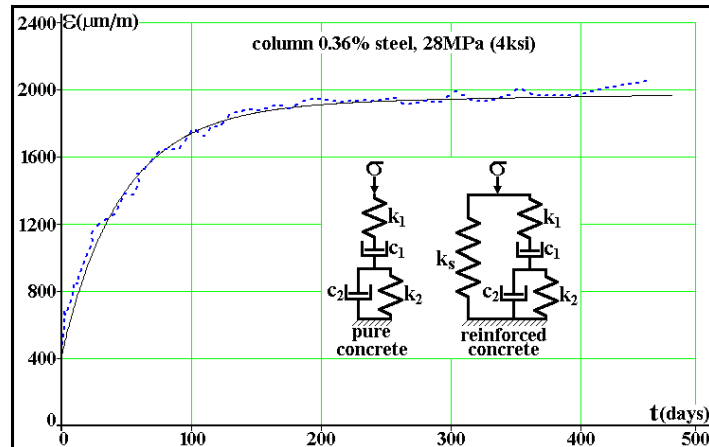


Figure 11: Strain history $\epsilon(t)$ for a $f'_c = 28\text{MPa}$ reinforced concrete column with steel area fraction $f_{a_s} = 0.36\%$, loaded by a fixed force that induces an initial strain $\epsilon_0 = 400\mu\text{m/m}$ ($k_1 = 24.87\text{GPa}$, $c_1 = 70\text{TPa}\cdot\text{day}$, $k_2 = 6\text{GPa}$ and $c_2 = 300\text{GPa}\cdot\text{day}$.)

296 elastic modulus) and a damper c_1 , in series with a Kelvin-Voigt element whose spring is k_2 and the
 297 damper is c_2 . The reinforcing steel is modeled by a spring k_s in parallel with the concrete. This model
 298 satisfactorily fitted creep data measured in reinforced concrete column obtained from the literature,
 299 demonstrating its potential to explain why the residual strains measured in instrumented rods of the

300 subway station columns were so high when compared with the nominal design strains. Therefore, this
301 procedure can be recommended to deal with similar load measurement problems.

302 Acknowledgements

303 Some of the authors have been partially supported by research scholarships provided by the Brazilian
304 National Research Council, CNPq.

305 References

- 306 [1] Vieira, R., Castro, J.T.P. & Freire, J.L.F., A new technique for measuring loads in concrete
307 columns. *Proceedings of the VI COTEQ*, 2002. In CD (in Portuguese).
- 308 [2] Leet, K., *Reinforced Concrete Design*. McGraw-Hill, 2nd edition, 1982.
- 309 [3] Buyukozturk, O., Creep and shrinkage deformation. *MIT 1054/1541 Mechanics and Design of*
310 *Concrete Structures Course Notes*, 2004.
- 311 [4] Levenberg, K., A method for the solution of certain non-linear problems in least squares. *Quarterly*
312 *of Applied Mathematics*, **2**, pp. 164–168, 1944.
- 313 [5] Marquardt, D., An algorithm for least-squares estimation of nonlinear parameters. *SIAM Journal*
314 *on Applied Mathematics*, **11**, pp. 431–441, 1963.
- 315 [6] Ziehl, P.H., Cloyd, J.E. & Kreger, M.E., Evaluation of minimum longitudinal reinforcement require-
316 ments for reinforced concrete columns. Technical Report Report FHWA/TX-02/1473-S, 1998.
- 317 [7] ACI, *ACI 209-R86: Prediction of Creep, Shrinkage, and Temperature Effects in Concrete Struc-*
318 *tures*, 1986.
- 319 [8] ACI, *ACI 318-95: Building Code Requirements for Reinforced Concrete and Commentary*, 1995.
- 320 [9] AASHTO - American Association of State Highway and Transportation Officials, Washington,
321 DC, *Standard Specification for Highway Bridges*. 15th edition, 1992.